JOURNAL OF MATERIALS SCIENCE 17 (1982) 499–507

The influence of crack depth on the fatigue crack propagation rate for a marine steel in seawater

B. F. JONES
Materials Department, Admiralty Marine Technology Establishment, Holton Heath, Poole, Dorset, UK

It has been shown that, for QIN steel specimens tested in seawater at a zero-tension cyclic frequency of 30 cycles per hour, crack growth rates are influenced by crack depth at low values of the stress intensity range (ΔK). Crack growth rates are faster for shallow cracks in the crack depth range 0.5 to 2.0 mm when ΔK is less than about 30 MN $m^{-3/2}$. For deeper cracks at low stress intensity ranges and for all crack depths at high stress intensity ranges, crack depth does not exert a significant influence on crack growth rate. The implications of such factors in relation to the provision of corrosion fatigue crack growth rate data for use in engineering design are discussed.

1. Introduction

The conjoint action of corrosion and cyclic stress on fatigue crack growth is of special interest in the application of structural steel in a marine environment. QIN is a weldable, medium strength steel developed to meet naval requirements, although its relevance to offshore engineering may increase if a need arises for higher strength steels than those currently employed (e.g. BS 4360 Grade 50D).

Fatigue crack growth rates are of special interest for predictions of life for large welded structures where the possible existence of crack-like defects in association with welds may eliminate the crack initiation phase. Crack growth rate per cycle, da/dN, is generally measured as a function of the crack tip stress intensity range (ΔK) to provide a means of applying data measured on a laboratory scale to large structures. Such an approach is compatible with the application of linear elastic or elastic–plastic fracture mechanics to fracture control and has, naturally, led to the use of similar specimens for both fatigue and fracture toughness testing. While standard methods for fracture toughness testing are well established [1–3], those for fatigue testing are at a much earlier stage [4] and only preliminary moves have been made toward standardizing corrosion fatigue testing.

It is the purpose of this paper to draw attention to some of the factors which must be considered in corrosion fatigue testing by reference to some results obtained on QIN steel.

2. Experimental procedure

2.1. Material

The composition, heat treatment and mechanical properties of the 38 mm thick QIN plate used in the study are shown in Table I.

2.2. Specimen

Tests were conducted on single edge-notched cantilever beam specimens which contained shallow tapered side-grooves (Fig. 1). The specimen was developed in conjunction with the Admiralty Marine Technology Establishment (AMTE) Flo-

TABLE I Composition, heat treatment and Mechanical Properties of QIN plate

Composition: Fe 0.17%C, 0.34%Mn, 0.21%Si, 0.014%S, 0.008%P, 2.36%Ni, 1.23%Cr, 0.34%Mo, 0.05%V, 0.08%Cu, 0.02%Al.	
Heat Treatment: Solution treated 2 h at 920° C, water quenched. Tempered 1½ h at 655° C, air cooled.	
Mechanical properties:	
0.2% proof stress	625 MN m^{-2}
Ultimate tensile stress	735 MN m^{-2}
Elongation (50.8 mm GL)	27%
Reduction of area	72%
Impact energy C_V:	
Upper shelf energy	157 J
Transition range	−89 to −125° C

0022–2461/82/020499–09$2.90/0

tation Fatigue Machine. The side-grooves were developed by experiment to produce straight fatigue crack fronts at all crack depths and thus avoid complications arising from crack front curvature. The orientation of specimens relative to the rolled plate is shown in Fig. 1.

Most specimens were precracked in air at a frequency of 200 cycles per minute (c.p.m.) to various depths using a constant-deflection, three-point-bend fatigue machine. During precracking the maximum stress intensities at the precrack tip were generally in the range 16 to 19 MN $m^{-3/2}$ and never exceeded 20 MN $m^{-3/2}$.

2.3. Fatigue tests

All tests were conducted in the AMTE Flotation Fatigue Machines [5], the principle of which is illustrated in Fig. 2. The load is applied to the specimen via a lever arm and pulleys by the weight contained in a bucket which is suspended in a tank. The load is removed from the specimen by filling the tank with water until the bucket floats; and applied by draining the tank. In practice, water is pumped between pairs of tanks at a rate selected to provide the required cyclic frequency. All of the tests discussed in this paper were conducted at a frequency of 0.5 c.p.m. (0.0083 Hz) using a trapezoidal waveform of the type shown in Fig. 3. For most tests the loading and unloading periods were about 15 sec each, although this time varied between 10 and 22 sec for the tests discussed here, depending on the load applied. Most tests were conducted using a zero to tension (R = minimum stress/maximum stress = 0) fatigue cycle. However, a few tests were conducted at a positive stress ratio (R = 0.5) where the minimum stress of the cycle was increased by use of a constant weight in the loading train, as illustrated on the left-hand side of Fig. 2.

Most tests were conducted in circulating, aerated natural seawater obtained weekly from the English Channel. Each batch of seawater was checked on receipt for salinity and pH to confirm that they were in the range 3.2 to 3.5% and 7.7 to 8.1, respectively. During a test the seawater was circulated through a rubber cup mounted around the notched region of the specimen. The temperature of the seawater ranged from 16 to 21° C depending on ambient conditions. The few data reported for air tests were obtained in laboratory

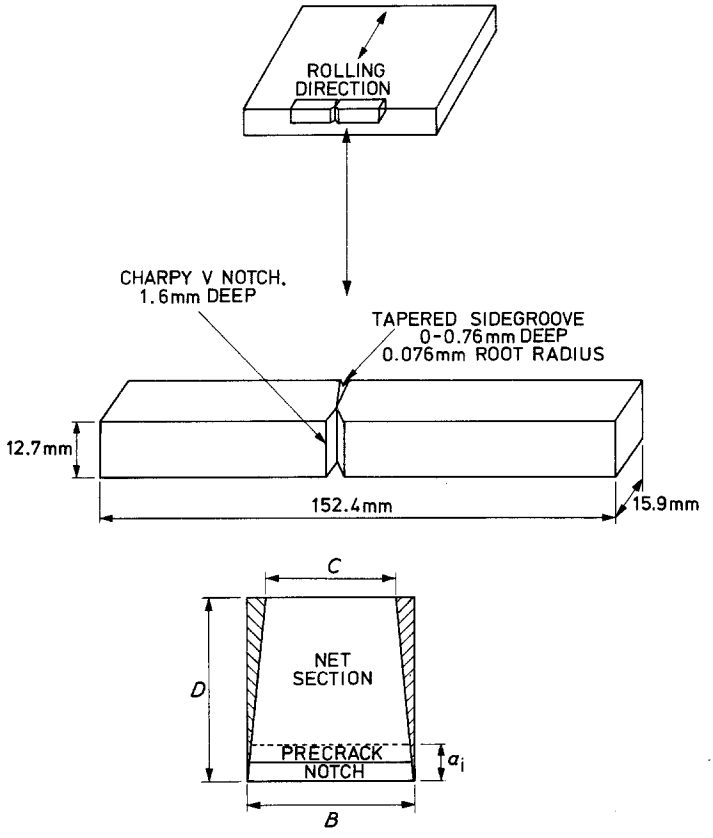

Figure 1 SEN cantilever beam fatigue specimen.

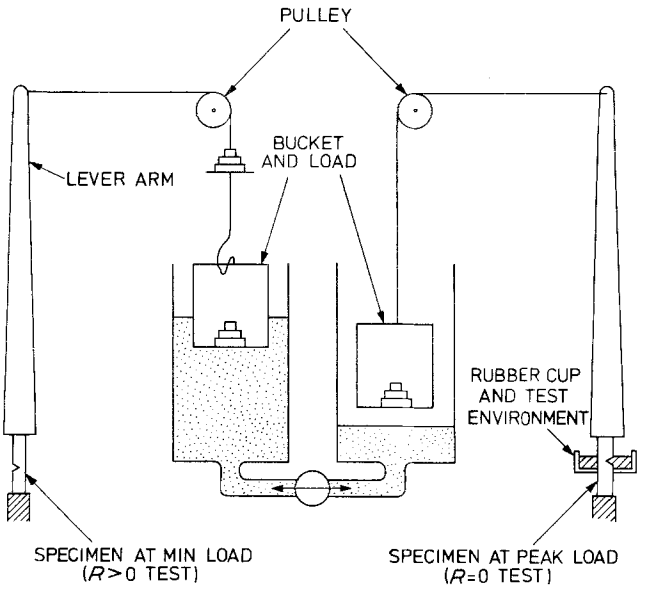

Figure 2 Schematic diagram of AMTE Flotation Fatigue Machines.

air, with no special control of humidity or temperature.

Crack depth was monitored using a direct current electrical resistance technique. A constant current of 20 A was supplied to the specimen on 2 to 4 occasions in every 24 h period, and the potential difference across the crack measured with a digital voltmeter. Calibration was achieved by growing fatigue cracks in several specimens to various potential differences, and then correlating these values with the appropriate measured crack depths after breaking the specimens in liquid nitrogen. The resolution of the system is estimated to be $\pm 2\,\mu V$, which corresponds to a crack depth of about $\pm$ 0.05 mm.

Stress intensities were calculated using Kies equation [6] which was slightly modified to account for the geometrical difference introduced by the tapered sidegrooves:

$$K_I = \frac{4.12M[(1-a/D)^{-3} - (1-a/D)^3]^{1/2}}{(B-0.1a)D^{3/2}}$$

where M = bending moment, a = crack depth (including notch) and all other symbols correspond to Fig. 1. Most tests were conducted under constant load conditions so that the maximum stress intensity for each cycle (K_{max}) increased continuously as the crack extended. Crack growth rates were determined by drawing tangents to plots of "crack depth" versus "number of cycles", and related to the crack tip stress intensity range ΔK.

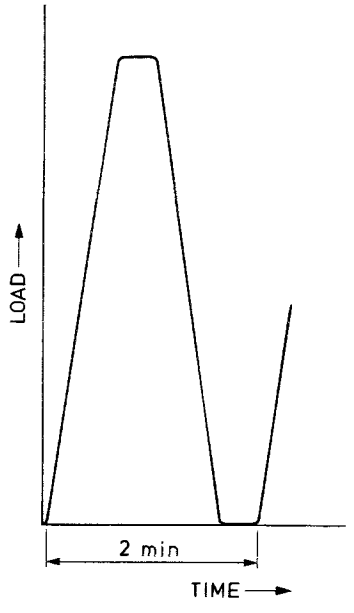

Figure 3 Trapezoidal waveform.

3. Results

Fig. 4 shows the crack growth rates measured on precracked specimens tested in air and seawater at $R = 0$ using various combinations of load and precrack depth (a_i) to provide several initial stress intensity ranges (ΔK_i). Some of the initial stress intensity ranges produced maximum stress intensities (K_{max}) which were below those employed in precracking, so crack growth rates during the first 0.2 mm of crack growth have been excluded from all the results shown in Fig. 4. This procedure has been adopted to eliminate crack growth rate measurements whilst the crack was growing in

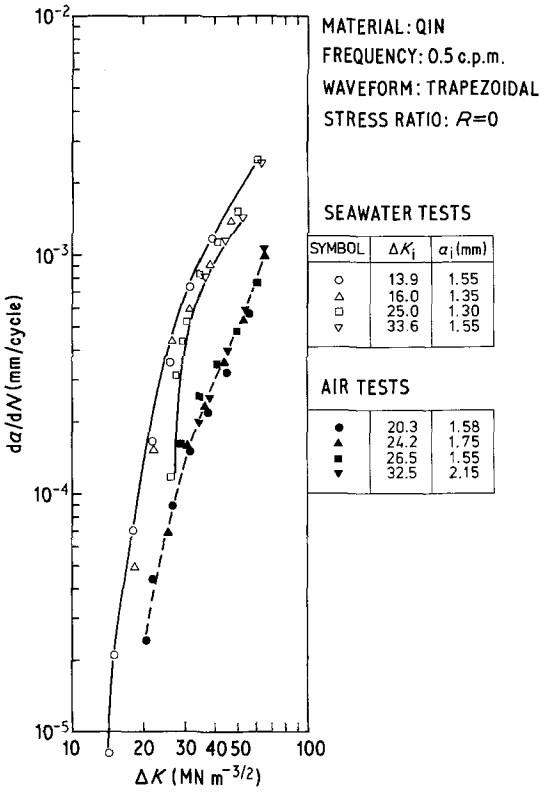

Figure 4 Crack growth rates for QIN steel in air and seawater from precracked specimens, excluding the first 0.2 mm of crack growth. Frequency 0.5 c.p.m., $R = 0$.

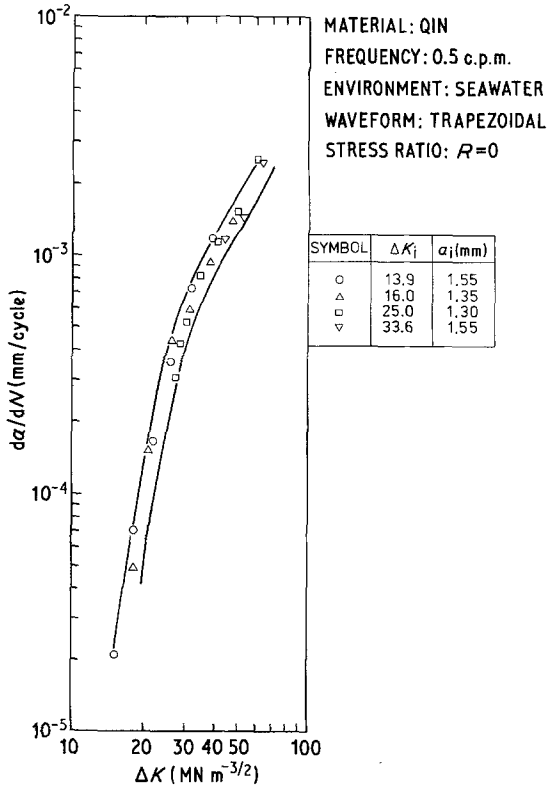

Figure 5 Crack growth rates for QIN steel in seawater from precracked specimens excluding the first 0.4 mm of crack growth. Frequency 0.5 c.p.m., $R = 0$.

the reverse plastic zone corresponding to precracking which was estimated for $K_{max} = 20\,MN\,m^{-3/2}$ to be 0.04 mm radius [7]. The air crack growth rates of Fig. 4 can be represented by a smooth curve with little scatter in the results. Seawater crack growth rates are faster than the air rates and also show much greater scatter at ΔK less than 30 MN $m^{-3/2}$, with higher growth rates at any given ΔK in this range for tests which had been commenced at lower initial stress intensities (ΔK_i).

The same seawater data have been replotted in Fig. 5, but in this case growth rates corresponding to growth within 0.4 mm of the precrack have been eliminated and the scatter at $\Delta K < 30$ MN $m^{-3/2}$ has been reduced.

Since the scatter in the seawater data of Fig. 4 cannot be attributed to the influence of the precracking reverse plastic zone size, and is absent in the case of air tests its seems likely that its occurrence is related to the influence of the seawater environment on the fatigue process, and suggests the existence of an "incubation" effect. In order to eliminate any possible influence of precracking procedure and the possibility that air trapped in the precrack might reduce the access of seawater to the crack tip, tests were conducted on specimens which had not been precracked. Notched specimens of the type shown in Fig. 1, which had not been precracked, were cycled at 0.5 c.p.m. in seawater using three load ranges. The results from these tests are compared with some of the results of Fig. 5, in Fig. 6. The test conditions employed in the specimens which had not beeen precracked are characterized by reference to the stress intensity calculated for a crack which has grown 0.1 mm from the notch. However, in line with the procedure adopted for Fig. 5, the first 0.4 mm of crack growth has not been used to generate growth rates. In Fig. 6 the results from precracked specimens which correspond approximately in terms of ΔK_i are used for comparison. Significantly faster crack growth rates were measured for specimens with shallower cracks at equivalent ΔK values, for example the crack growth rates for specimens with cracks between 0.5 and 1.0 mm deep were about 4 times faster than those measured on specimens with cracks between 2.0 and 2.5 mm deep. However, as ΔK increases, the difference in growth rate

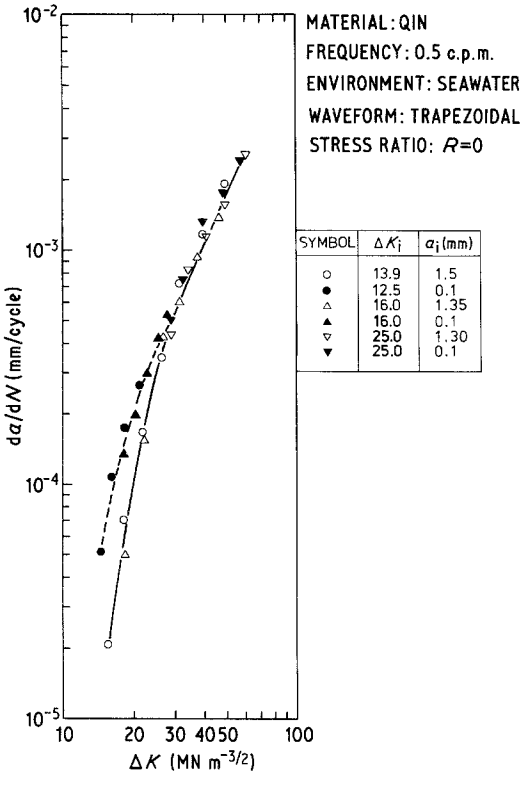

Figure 6 Comparison of crack growth rates for QIN steel in seawater obtained from specimens with and without precracks (for both types of specimen the first 0.4 mm of crack growth are excluded). Frequency 0.5 c.p.m., $R = 0$.

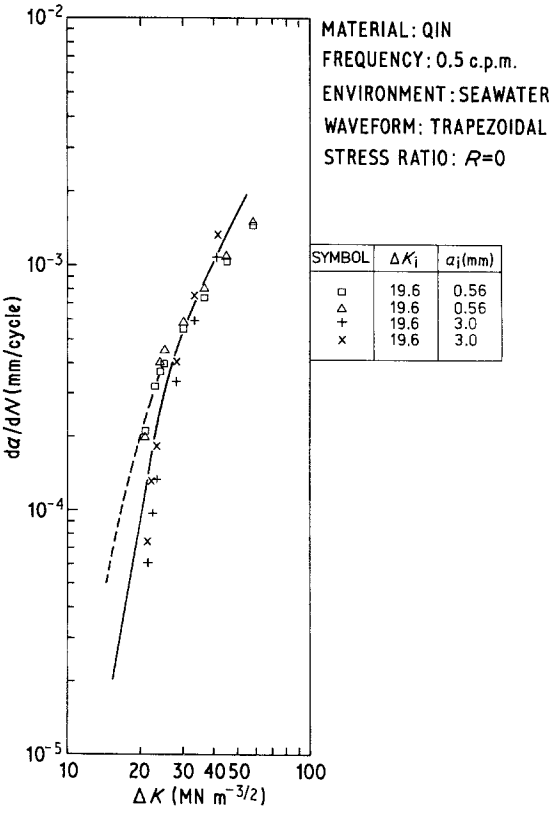

Figure 8 Comparison of crack growth rates for different initial crack depths for specimens in which notch plus precrack depth is constant. Frequency 0.5 c.p.m., $R = 0$, Environment: seawater.

between deep and shallow cracks reduces until at $\Delta K \sim 30$ MN m$^{-3/2}$ crack growth rate is relatively independent of crack depth in the range 0.5 to 6.0 mm.

A further series of tests was conducted in which crack growth rates measured on specimens with very deep (3.0 mm) precracks were compared with the growth rates measure on specimens with shallow (0.5 mm) precracks but containing deep notches (i.e. notch + crack depth equal for all specimens, see Fig. 7). The results of duplicate tests under identical conditions are compared with the curves for "shallow" and "deep" cracks from Fig. 6 in Fig. 8. Crack growth rates for the very deep precrack are similar or slightly slower than those recorded in normal tests, whilst those for specimens with deep notches but shallow precrack are similar to those measured on specimens which had not been precracked. Fig. 9 compares the crack + notch depth versus number of cycles for the two types of specimen shown in Fig. 7, to demonstrate the large effect which the differences in crack geometry have on specimen life.

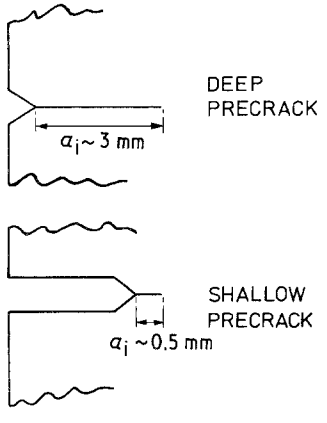

Figure 7 Notch/precrack configuration for comparison of crack growth rates in specimens with deep and shallow precracks but identical notch plus precracks lengths.

In Fig. 10 the growth rates obtained from tests where low ΔK has been achieved by load reduction are compared with the curves for "shallow" and "deep" cracks from Fig. 6. For the load reduction tests the initial crack depth and stress

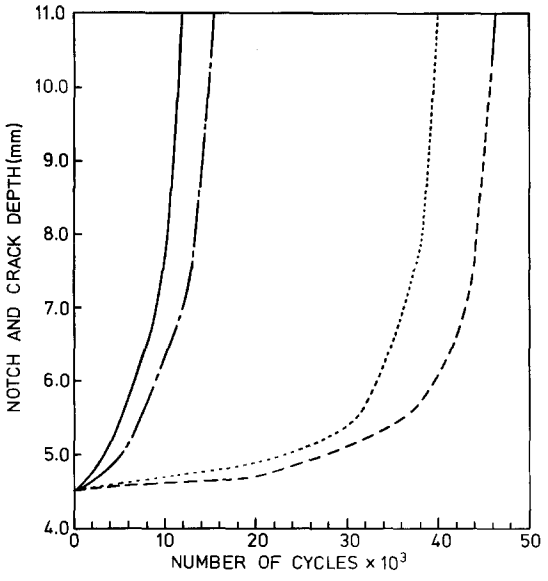

Figure 9 Notch plus precrack depth versus number of cycles for specimens with different precrack depths. ———, $a_i = 0.56$; —·—, $a_i = 0.56$; ·····, $a_i = 3.00$; - - - - -, $a_i = 3.00$.

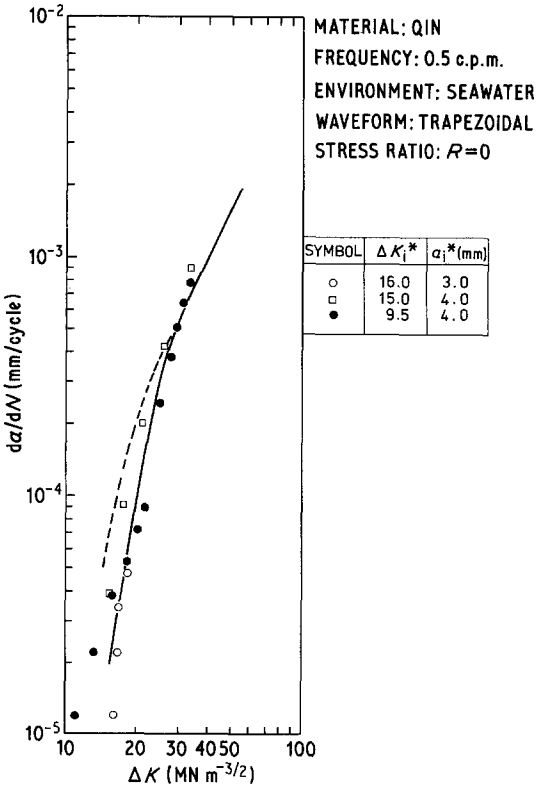

Figure 10 Crack growth for QIN in seawater obtained by load reduction tests. Frequency 0.5 c.p.m., $R = 0$.

intensity range refer to the values which prevail at the point when the new (lower) load comes into operation and are denoted by the inclusion of an asterisk (i.e. a_i^*, ΔK_i^*) to distinguish these values from the initial values quoted in constant-load amplitude tests. Due account has been taken of the reverse plastic zone size corresponding to the previous (higher) load and crack growth within the prior plastic zone has been ignored. Although the nature of these tests dictates that the growth rates measured correspond to very deep cracks, it is noted that some of the rates measured are faster than those recorded in normal tests with shorter cracks.

Fig. 11 shows that the crack growth rates are independent of crack depth at low ΔK when tests are conducted at a stress ratio of 0.5 rather than $R = 0$, and that the rates measured correspond to those determined for "shallow" cracks at $R = 0$.

4. Discussion

The form of the da/dN versus ΔK curve determined for QIN steel in seawater shows a feature which is not usually evident in the crack growth rate curves published for steels. Reference is usually made to three main regions in the relationship, as illustrated in Fig. 12a, i.e. the threshold region at low ΔK, the linear mid-range region which can be represented by a Paris–Erdogan equation [5], and a region where the growth rate accelerates just below the critical stress intensity for the specimen. However, for QIN steel in seawater an inflection in the curve is noted at $\Delta K \sim 30$ MN $m^{-3/2}$, well above the threshold region which occurs at $\Delta K < 10$ MN $m^{-3/2}$ (for example see Fig. 10 where growth rates $> 10^{-5}$ mm $cycle^{-1}$ are recorded at $\Delta K = 11$ MN $m^{-3/2}$). Although the data are more accurately represented by a smooth curve, it can be approximated by two equations of the Paris–Erdogan type (as shown schematically in Fig. 12b), the slope of the line at higher ΔK being less than that for the line at lower ΔK. Vosikovsky [9] has reported a similar inflection in data he obtained for HY130 steel tested under similar conditions.

It is probably significant that crack depth ceases to be an important factor for $\Delta K > 30$ MN $m^{-3/2}$, where the inflection occurs. Tomkins [10] differentiates between the crack growth processes which occur at high and low ΔK levels. He suggests that Stage I growth [11] occurs at low ΔK levels, where the crack tends to grow within the operating flow line leading to a tortuous crack path, and Stage II growth occurs at higher ΔK when the

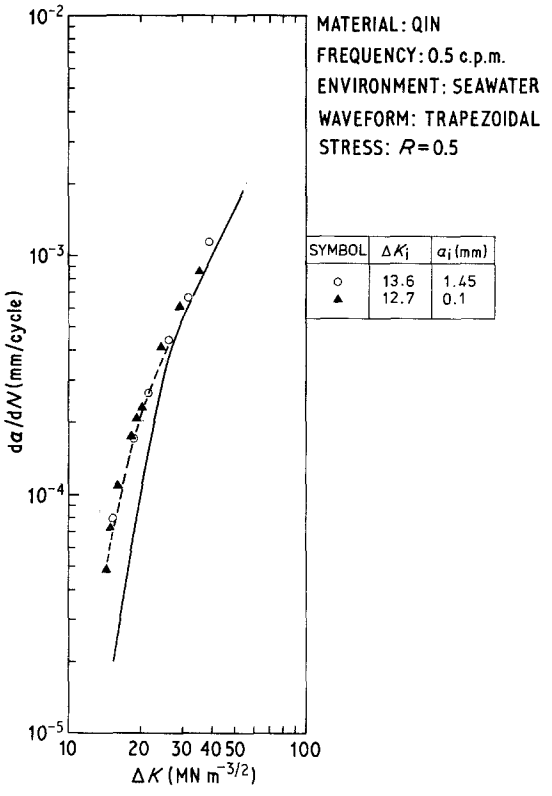

Figure 11 Influence of initial crack depth on crack growth rates for QIN in seawater at a stress ratio (R) of 0.5. Frequency 0.5 c.p.m.

crack grows normal to the applied stress by the mechanism which leads to the formations of striations. The transition between the two mechanisms of crack growth is thought to depend on the relationship of the opening at the crack tip to the discrete dislocation structure in the region of the crack tip [12], and seems likely to occur in QIN steel in the ΔK range 10 to 30 MN $m^{-3/2}$. Tomkins suggests that the access of the environment to the crack tip might be considerably restricted during Stage I when the crack opening is small and the crack path tortuous, such restriction diminishing as crack opening increases and the crack path straightens at higher ΔK during Stage II growth. Under circumstances where the access of the environment is restricted it seems reasonable to expect that crack depth will have a significant effect on the crack growth process. Even if physical access of the environment to the crack tip was not a problem, the rate of diffusion of species from the bulk solution to the crack tip, when crack opening is small and the volume of solution within the crack enclave correspondingly small, may represent an important rate-controlling factor. Such factors have previously been discussed in relation to corrosion fatigue [13] and fatigue in the presence of water vapour [14, 15], and may be relevant to other observations of crack depth effects [16, 17], but their implications in terms of fatigue test methods have not been elucidated. The problem is further complicated by the difficulties in quantifying the effects because the effects of pumping action, turbulence and surface roughness are difficult to include. However, in qualitative terms an effect of crack depth at low ΔK and small crack opening would be expected from the arguments advanced above.

Consideration has been given to the fact that some of the measurements of crack growth rates in the present work involves near-notch conditions. In this respect it has been convenient to adopt the precaution of ignoring the first 0.4 mm of crack growth in all tests since no growth rate (or stress intensity) is quoted for a crack shorter than 0.4 mm, whereas the extent of the notch tip strain

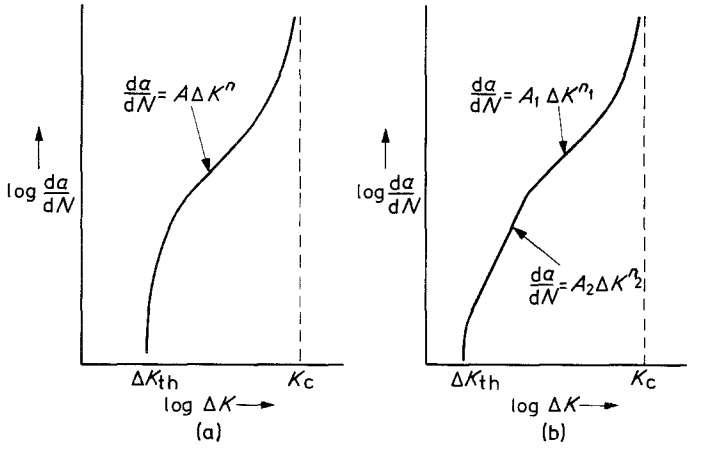

Figure 12 Schematic representation of da/dN versus ΔK relationships. (a) Typical fatigue crack growth curves; (b) form of curve for QIN in seawater at 0.5 c.p.m.

field is estimated to be only 0.1 mm [18]. It also appears unlikely that residual machining stresses associated with notching are of importance since the data of Fig. 13 were obtained for specimens given stress relieving treatments of 1 h at 600° C before or after notching, and show no significant difference in growth rate. The procedure of heat treating specimens before and after notching was adopted because it had been demonstrated that the stress relieving treatment itself has an influence on corrosion fatigue crack growth rate [19].

It is evident from the foregoing that the influence of crack depth on crack growth rate is significant only for shallow cracks and once the depth exceeds about 2 mm there ceases to be any futher reduction in growth rate. However, the load reduction results shown in Fig. 10 indicate that it is possible to obtain crack growth rates approaching those for shallow cracks even in very deep cracks under these special circumstances, illustrating that specimen history can exert an important influence. The fact that crack depth has no influence even at

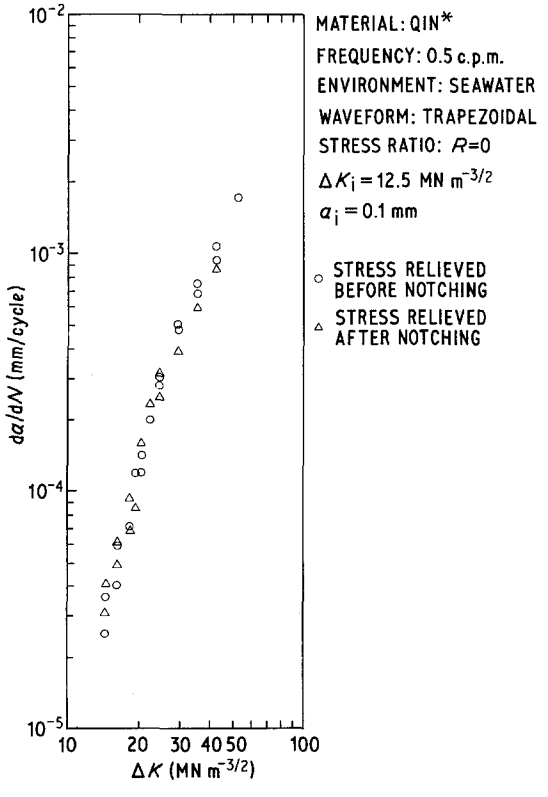

Figure 13 Influence of stress relief (1 h at 600° C, air cool) on crack growth rates for QIN in seawater. Frequency 0.5 c.p.m. $R = 0$, $\Delta K_i = 12.5$ MN m$^{-3/2}$, $a_i = 0.1$ mm. 0, Stress relieved before notching, Δ, stress relieved after notching.

$\Delta K \sim 15$ MN m$^{-3/2}$ in tests conducted at $R = 0.5$ (Fig. 11) lends support to Tomkin's suggestion [10] that the influence of positive stress ratios in increasing crack growth rates at low ΔK is related to the improved access of environment to the crack tip as a result of the increased crack opening (N.B. for $\Delta K = 15$ MN m$^{-3/2}$ at $R = 0.5$, $K_{max} = 30$ MN m$^{-3/2}$ and crack tip opening $\propto K^2_{max}$). Thus in the $R = 0.5$ tests performed, K_{max} has always been greater than the value required to produce Stage II crack growth, and good access of the environment. It is worth noting however that at lower ΔK values in positive stress ratio tests access of the environment would still be restriced by low crack opening.

It is apparent from these results that under certain experimental conditions crack depth can exert a significant influence on corrosion fatigue crack growth. The degree of influence will depend on the material and environment as well as the other conditions discussed above. Most fracture-control plans consider the growth of shallow surface-breaking defects as an important factor in their analyses, and employ "upper-bound" crack growth rates to provide conservative predictions of fatigue life. Crack growth rates are often measured in the laboratory using fracture mechanics-type specimens, and the tendency is to use specimens of sufficient thickness to provide plane strain conditions. The advice of the ASTM test method [3] is that the minimum precrack length should be 10% of the specimen thickness, with no upper limit on precrack length. Further the trend in corrosion fatigue crack growth studies is to produce data in the low crack growth regime at low ΔK to provide relevant design data. Thus there is an inherent danger that the use of specimens with deep precracks could lead to serious overestimates in fatigue life predictions, unless special care is exercized in providing true "upper-bound" growth rates.

5. Conclusion

Faster crack growth rates were recorded at equivalent ΔK levels for tests in seawater of QIN steel specimens containing shallow cracks compared to specimens containing deep cracks. Significantly faster rates were measured for crack depths less than about 2 mm when ΔK was below 30 MN m$^{-3/2}$ and $R = 0$. It is also noted that specimen stress history can exert an important influence on crack growth rate, load reductions leading to faster

crack growth rates at low ΔK even in specimens containing deep cracks. Such factors require careful consideration in relation to the provision of corrosion fatigue crack growth rate data for use in engineering design.

Acknowledgements

Mr D. E. McGeachie designed and commissioned the AMTE Flotation Fatigue Machines and together with Mr V. Reynolds made a significant contribution to the planning and organization of the experimental programme. The contribution of Mr D. Fraser and Mr K. Turner to the experimental programme is gratefully acknowledged, as is the assistance of many colleagues at AMTE (Holton Heath) and AMTE (Dunfermline).

References

1. British Standard number BS 5447:1977.
2. British Standard number BS 5762:1979.
3. American Society for Testing of Metals Publication number ASTM E 399:74 (American Society for Testing of Metals, Philadelphia, 1974).
4. American Society for Testing of Metals Publication number ASTM E 647-78T (American Society for Testing of Metals, Philadelphia, 1978).
5. D. E. McGEACHIE, M.Phil thesis, University of Southampton (1975).
6. B. F. BROWN, *Mater. Res. Stand.* **6** (1966) p. 129.
7. H. H. JOHNSON and P. C. PARIS, *Eng. Fracture Mechanics* **1** (1968) 3.
8. P. C. PARIS and F. ERDOGAN, *J. Basic Eng., Trans. ASME* **D85** (1963) 528.
9. O. VOSIKOVSKY, *J. Testing Evaluation* **6** (1978) 175.
10. B. TOMKINS, Paper C111/77, Proceedings of the Conference on The Influence of Environment on Fatigue, London, May 1977 (The Institution of Mechanical Engineers, London, 1977).
11. P. J. E. FORSYTH, Proceedings of Crack Propagation Symposium, Cranfield (1961) p.76.
12. R. J. H. WANHILL, *Met. Trans* **6A** (1975) 1587.
13. R. HOLDER, Paper C102/77, Proceedings of the Conference on The Influence of Environment on Fatigue, London, May 1977 (The Institution of Mechanical Engineers, London, 1977).
14. P. S. PAO, W. WEI and R. P. WEI, in "Environment Sensitive Fracture of Engineering Materials" (edited by Z. A. Foroulis) (TMS-AIME 1979) pp. 565–80.
15. R. P. WEI, P. S. PAO, R. G. HART, T. W. WEI and G. W. SIMMONS, *Met. Trans.* **11A** (1980) 151.
16. S. PEARSON, *Eng. Fracture Mechanics* 7 (1975) 235.
17. P. CHAUHAN and B. W. ROBERTS, *Metall. Mater. Technol.* **11** (1979) 131.
18. R. A. SMITH and K. J. MILLER, *Int. J. Mechanical Sci.* **19** (1977) 11.
19. AMTE, data to be published in *Int. J. Fatigue*.

Received 9 March
and accepted 14 July 1981